






# Development of Myoelectric Control Module for Prosthetic Hand with Artifact Removal during Sensory Electrical Stimulation

Yashuo Yu<sup>1</sup><sup>a</sup>, Chih-Hong Chou<sup>1,2</sup><sup>b</sup>, Jie Zhang<sup>1</sup><sup>c</sup>, Manzhao Hao<sup>1,2</sup><sup>d</sup> and Ning Lan<sup>1,2</sup><sup>e</sup>

<sup>1</sup>*School of Biomedical Engineering, Shanghai Jiao Tong University, Shanghai, China*

<sup>2</sup>*Institute of Medical Robotics, Shanghai Jiao Tong University, Shanghai, China*

**Keywords:** Prosthetic Hand, Sensory Feedback, Transcutaneous Electrical Nerve Stimulation (Tens), Stimulation Artifact.


**Abstract:** Evoked Tactile Sensation (ETS) with transcutaneous electrical nerve stimulation (TENS) can provide amputees with a non-invasive neural interface for sensory feedback. However, sensory stimulation at the projected finger map (PFM) on the stump skin causes interference in surface electromyographic (sEMG) signals used for prosthesis control. This study developed a practical solution that combined hardware blanking and software filtering to eliminate stimulus artifacts in real-time. A synchronized blanking circuit was inserted after the differential amplifiers to partially remove artifact spikes. EMG signal was then sampled and further processed by a digital signal processor (DSP). A digital comb filter removed the remaining artifacts at all harmonic frequencies of stimulation. The filtered EMG was rectified, and its envelope was extracted to control prosthetic hand. This technique was tested for its effectiveness in removing stimulus artifacts in three able-bodied subjects and in one transradial amputee operating a Bebionic hand. Results in able-bodied subjects indicated that the technique was effective in removing stimulus artifacts in EMG under different conditions. In the amputee subject, grasp control using the Bebionic hand was obtained with simultaneous sensory stimulation in the ipsilateral stump. The amputee subject achieved an average success rate of 90% for identifying the length of grasped objects. Tests confirmed that the technique is adequate to remove stimulus artifacts from EMG signals and allows control of the Bebionic hand with simultaneous sensory stimulation.


## 1 INTRODUCTION


Commercial prosthetic hands employ surface electromyographic (sEMG) signals from residual muscles for motor control. However, a survey of amputees reported that the low prevalence and high abandonment rate of such devices are attributed to the lack of sensory function (Smail et al., 2021), which plays an important role in the daily activities (e.g. grasping tasks) for able-bodied subjects (Johansson & Flanagan, 2009). Although there have been many studies on closed-loop prosthetic systems in recent years, the progress has been limited in the laboratory (Bensmaia et al., 2020). Therefore, the restoration of sensory function of a myoelectric-controlled bionic hand has been a great challenge in neural engineering.


Our previous studies established that sensory feedback delivered with transcutaneous electrical nerve stimulation (TENS) to the projected finger map (PFM) of the amputated stump can generate evoked tactile sensation (ETS), and revealed that PFM on the stump skin of the forearm of amputees corresponded to the projection of the whole hand (Chai et al., 2015). This afferent information shares a natural and direct pathway with intact tactile afferents to the primary somatosensory cortex (SI) (Hao et al., 2020). The finger-specific perceptibility affords the advantage of multi-facet recognition during prosthetic grasping (Li et al., 2021).


In a closed-loop myoelectric prosthesis with non-invasive sensory stimulation by TENS, it also requires to collect sEMG signals for motor control,

<sup>a</sup>  <https://orcid.org/0000-0003-3512-4954>

<sup>b</sup>  <https://orcid.org/0000-0002-8985-5050>

<sup>c</sup>  <https://orcid.org/0000-0002-6075-2074>

<sup>d</sup>  <https://orcid.org/0000-0001-8744-7128>

<sup>e</sup>  <https://orcid.org/0000-0001-6061-5419>

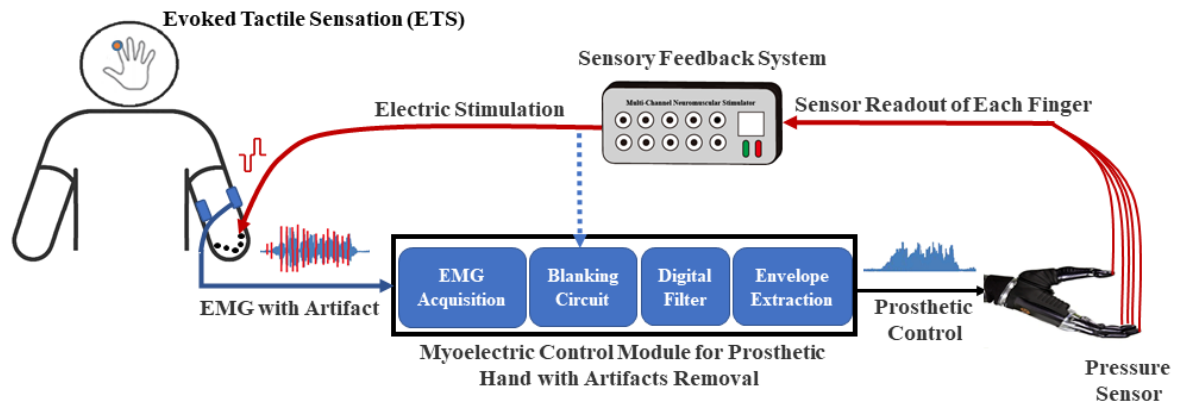


Figure 1: System block diagram of the integrated myoelectrical control and ETS-based sensory feedback of a Bionic prosthetic hand.

where the placement location of sEMG sensors and stimulation electrodes are very close to each other at the stump ipsilaterally. Stimulation artifacts conducted through the skin and muscles can produce a stimulus artifact much larger than EMG signals from voluntary contractions. Accordingly, a major drawback of TENS applied to the stump skin is that it generates interference to sEMG signals.

A simple way to handle EMG contaminated with stimulus artifacts from hardware is to wait for the recovery of EMG amplifiers from saturation, which requires a fast recovery of electronic components or to switch off the amplifier (mute) when the stimulus pulse starts to be delivered and discard the data during saturation (Schauer et al., 2004). Besides, sample and hold circuit can also be used for removal by storing the DC levels before the pulse and holding it during the pulse (Babb et al., 1978).

Software-based approaches combining embedded processors allow for real-time or semi-real-time removal. Software algorithms for real-time processing need not only to achieve further enhancements than hardware processing but also to ensure instantaneity, which requires appropriate complexity. However, most of algorithms for post-processing focus on improving the algorithm accuracy instead of efficiency. The software methods for suppressing EMG signal artifacts can be broadly classified into the following categories according to the existing research: 1) blanking (Yi et al., 2013; Li et al., 2019), 2) comb filter (Frigo et al., 2000; Widjaja et al., 2009), 3) adaptive filter (Qiu et al., 2015), and 4) other methods (Yochum et al., 2014; Pilkar et al., 2016; Bi et al., 2021).

Dosen et al. (Dosen et al., 2014) used a time-division multiplexing (TDM) approach with similar logic to sample and hold, performing stimulation and recording in dedicated, non-overlapping time

windows to avoid interference, and thus building a real-time closed-loop control system.

The various solutions of artifacts removal are not readily available for practical use in closed-loop control prosthetic systems. In this study, we developed and tested a module composed of a hybrid method of hardware blanking and software filtering to remove stimulus artifacts in sEMG caused by TENS. This technique can allow integration of control of myoelectrical prosthesis with the ETS-based sensory feedback in the ipsilateral stump of amputees. We verified this method with a commercially available Bionic hand to form a closed-loop system. Test results indicated that the prosthesis works properly with simultaneous sensory perception of grasp, demonstrating that sensory feedback adds the functionality of the device. The system block diagram is shown in Figure 1. The blue line represents control pathway, and the red line represents sensory feedback pathway.

## 2 METHODS

### 2.1 Module Overview

The framework of the myoelectric control module for prosthetic hand with artifact removal is shown in the block diagram in Figure 2. In the control pathway, the EMG signals from residual muscles are collected with surface electrodes. The signals are blanked (switch off) by a hardware circuit during stimulation and filtered to remove the remaining artifacts. The processed EMG signals are rectified, and the envelopes are used to control the opening and closing of prosthetic hand. EMG sampling, artifact filtering, rectifying and envelope extraction are all processed in

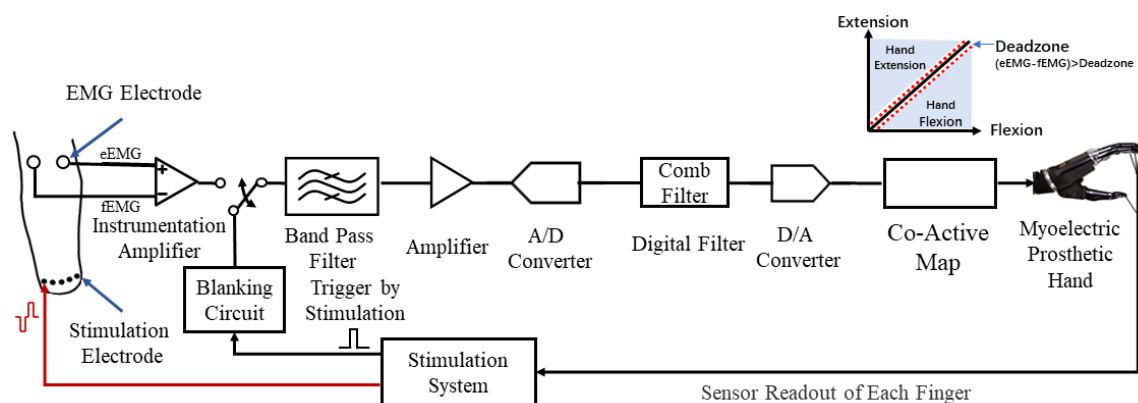


Figure 2: The hardware block diagram of the myoelectric control module.

a digital signal processor (DSP). In the sensory pathway, contact pressures at prosthetic fingertips are converted to a pattern of electrical stimuli and delivered to five stimulation electrodes via the multi-channel stimulator, which can generate specific stimulation patterns according to an encoding protocol. The stimulation patterns are charge-balanced biphasic rectangular pulse trains with positive pulses going first. Sensory intensity is modulated by pulse amplitude (PA), pulse frequency (PF) and pulse width (PW). Changes in stimuli parameters can cause different sensory modalities, as in (Yang et al., 2020).

## 2.2 System Description

To reduce the effect of the electrical stimulus on the signal acquisition, we designed a blanking circuit to turn off the electrical stimulus input to avoid the current saturating the capacitor. We also moved the switch to the output of the instrumentation amplifier (OPA2333, Texas Instruments, USA) for reducing the signal noise during switching (Rolston et al., 2009). The architecture of the system is shown in Figure 2.

When grasping occurs, the sensor in the prosthetic hand generated the electrical stimulation signal. The output of the stimulation sent the electrical stimulation trigger to the blanking circuit simultaneously. Then, the system turned off the meter amplifier output within 10  $\mu$ s, and conversely turned on the acquisition function within 10  $\mu$ s after the electrical stimulation ends.

The subsequent part is a typical EMG signal processing circuit. After band-pass filtering and A/D conversion, the signal was processed with the comb filter (refer to details in Section 2.3) implemented by DSP. Then, the EMG envelope features were extracted. Finally, the signal through co-active

mapping of one pair of antagonistic muscles was used as the output control of the prosthesis. In addition, a dead zone was set to avoid driving prosthesis under weak EMG, which may lead to frequent jitter.

## 2.3 Signal Processing

After being propagated as local currents, stimulation pulses manifest in the frequency domain as a fundamental wave of the pulse delivery frequency and its higher harmonics, which can be removed with a comb filter with the following equation,

$$y(n) = \frac{x(n) - x(n - N_{Tstim})}{\sqrt{2}} \quad (1)$$

where  $x(n)$  and  $y(n)$  are for the raw and the filtered EMG at sampling time  $n$ .  $N_{Tstim}$  is the number of samples between inter-pulse-intervals (IPIs). The scale factor  $\sqrt{2}$  can keep the signal power constant after filtering (Frigo et al., 2000).

Then EMG signals were then filtered through a 6th Butterworth lowpass filter with a 400 Hz cutoff frequency to reject high frequency components. Finally, the signals were rectified and filtered with 2nd lowpass Butterworth with 10 Hz cutoff to extract envelope curves.

All filters were implemented on a DSP (STM32H743, STMicroelectronics, Italy) to provide real-time operation.

## 3 EXPERIMENTS

### 3.1 Subjects

Three able-bodied subjects (2 males and 1 female, 29 $\pm$ 6.083 yrs.) and 1 transradial amputated subject (male, 54 years old, left amputation) were recruited to

participate in this study. All the experiment protocols were approved by the Institutional Review Board for Human Research Protections, Shanghai Jiao Tong University.

### 3.2 Experiment Setup

The subject was seated at a table, and a Bebionic hand (Otto Bock HealthCare) was fixed with an upright tripod. Two pairs of bipolar EMG electrodes (Norotrode 20 Bipolar sEMG Electrodes) were placed on ulnar/radial side of forearm near elbow end to capture two-channel EMG signals of wrist flexor/extensor. The prosthetic hand was set to close when the flexor contracted and to open with extensor contraction (Figure 3 (a)). A non-invasive stimulation pattern generator (Liu et al., 2015), delivered five channels of TENS to five metal stimulation electrodes on the forearm skin (Figure 3 (b), (c)) for able-bodied subjects or the stump PFM site (for amputees) corresponding to pressures (measured by force sensor, FlexiForce A201, Tekscan, Inc., USA) on each digit tip (Figure 3 (d)). The stimulation electrode was a disk Ag/AgCl electrode with 10 mm diameter, custom made by the Institute of Semiconductors of the Chinese Academy of Sciences. The reference electrode (non-woven fabric circular electrode with 5 cm diameter) of each channel was placed near the olecranon. The system equipped with EMG acquisition function can output two channels of co-active mapped execution signals to manipulate the prosthesis. Both stimulation and EMG processing were controlled by a host PC with self-innovate software designed by C#. The two-channel EMG signals were sampled at 2 kHz.

### 3.3 Experiment Protocols

There were two experiments in total. In the first experiment, the able-bodied subjects explored whether artifact removal strategies were effective under different settings, and the second experiment was carried out to verify the ETS-based sensory feedback in real-time for closed-loop control on amputees, which can be seen as a variant of (Li et al., 2021) but in ipsilateral.

The 50 Hz fixed stimulation frequency was used throughout the experiment, while pulse amplitude (PA) and pulse width (PW) were modulated to encode prosthetic hand contact pressure (Yang et al., 2020).

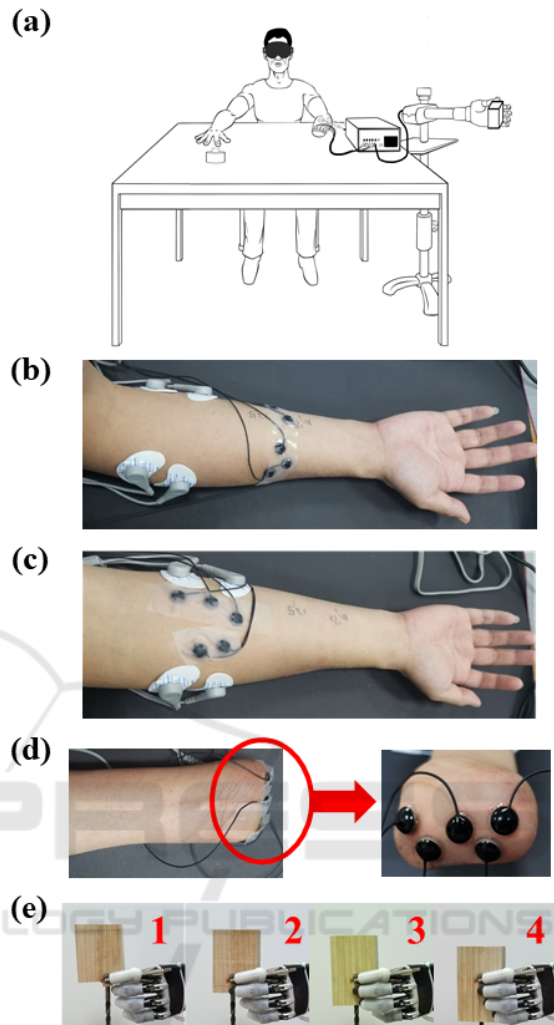


Figure 3: (a) Experiment scene. (b) and (c) show far and near electrode distances respectively on able-bodied subjects while (d) shows the amputee's electrode sites with stimulation electrodes on PFM. (e) 4 blocks of different lengths (VS, S, M, and L) used in experiment 2, allowing contact of different numbers of fingers. Fingers involved in pinch are, from left to right: thumb and index; thumb, index and middle; thumb, index, middle and ring; thumb, index, middle, ring and little.

### 3.4 Experiment 1: Filtering Algorithm Validity Test

There were two conditions of stimulation electrode placement: 1) far condition: stimulation electrodes were placed between one half and three quarters (distal end) of the full length (measured by the distance from olecranon to ulnar styloid process) of the forearm far from the EMG electrodes (Figure 3 (b)); 2) near condition: between two EMG electrodes

(Figure 3 (c)). The former condition was determined according to the actual length of amputees' residual limb. The stimulation intensity level was set with a PW of 600 $\mu$ s per channel. Then the PA of each channel was set to the upper limit value of buzz sensation multiplied by 0.8 when 5 channels delivering simultaneously to avoid uncomfortableness.

The experimental task was designed to meet the practical application of the prosthetic for hand opening and closing movement. The subjects recorded their EMG by flexing/extending their wrist for about 2s with stimulation. Ten trials for each combination of electrode distances and flexion/extension, that was 40 trials in total for each subject.

Power generated by stimulus artifacts was further quantified. First, EMG of able-bodied subjects was segmented, and each segment contained 4000 sample points (2 s signal sampled at 2 kHz). Then the power spectral densities (PSD) were calculated by Welch's method. Eventually the PSD at each artifact harmonic with 10Hz on each side was accumulated to estimate the artifact power ( $P_{stim}$ ) with Eq. (2),

$$P_{stim} = \sum_{k=1}^{fs/(2*f_{stim})} \sum_{i=k*f_{stim}-10}^{k*f_{stim}+10} PSD(i) \quad (2)$$

where  $k$  is the number of harmonics and  $i$  is the specific value of the discrete spectrum.

The averaged  $P_{stim}$  in every condition over all subjects was calculated. And the electrode distance was considered as an intra-class factor to compare the mean  $P_{stim}$ , whose significant differences were tested with two-tailed paired Tukey's honestly significant difference test.

### 3.5 Experiment 2: System Operation Validation Test

In experiment 2, a response button was placed on amputated subject's contralateral hand. The experimental task was to bend the wrist so that the prosthetic hand can touch the wooden block when closing. There were 4 different lengths of the blocks, which could be represented by VS (very small), S (small), M (medium), and L (large) respectively. Hence, the number of fingers varied when the hand grasped the block (Figure 3 (e)). During the contact process between the prosthetic hand and the wood block, the subject needed to determine the block size

by the finger numbers feeling through ETS. 5 channels of pressure signals, prosthetic hand aperture (distance between tips of thumb and index), and the response signal was sampled at 100 Hz synchronized with EMG. Each grasping and identification make a single trial and the experiment contained 40 trials in total, with 10 trials for each size pseudo-random ordered.

## 4 RESULTS

### 4.1 Effects of Artifact Removal at Different Stages

The representative EMG signals at each processing stage are plotted in Figure 4. Raw EMG without any blanking is contaminated by a large amplitude of stimulus artifacts with 1 channel of stimulation at 1 mA 200  $\mu$ s. The artifacts do not saturate the differential amplifiers. It is clear that artifacts are significantly diminished with hardware blanking. It is noted, however, that recording electrodes place nearer to the stimulation electrodes yield fewer artifacts than those with greater distance. Moreover, contaminated EMG signals display artifact components in all harmonic frequencies. After processing by the comb and Butterworth filters, artifacts of all harmonic components are largely invisible in the filtered EMG. In spite of some loss of EMG components at the harmonic frequencies, the envelope of processed EMG signals can still be extracted.

### 4.2 Filtering Algorithm Validity Results

Figure 5 summarizes results across different conditions in three able-bodied subjects. The vertical axis shows spectral power in dB. Statistic analysis indicates that  $P_{stim}$  decreased along artifacts removal stages regardless of muscle and the distance between EMG and stimulation electrodes. It is clear that each stage of hardware and software processing of this method results in a certain degree of removal of artifact components from the contaminated EMG. It is expected that, artifacts power was the largest with no blanking; and artifacts power is the smallest with blanking and digital filtering. Artifacts are stronger for EMG recording electrodes placed farther away from the stimulation electrodes.

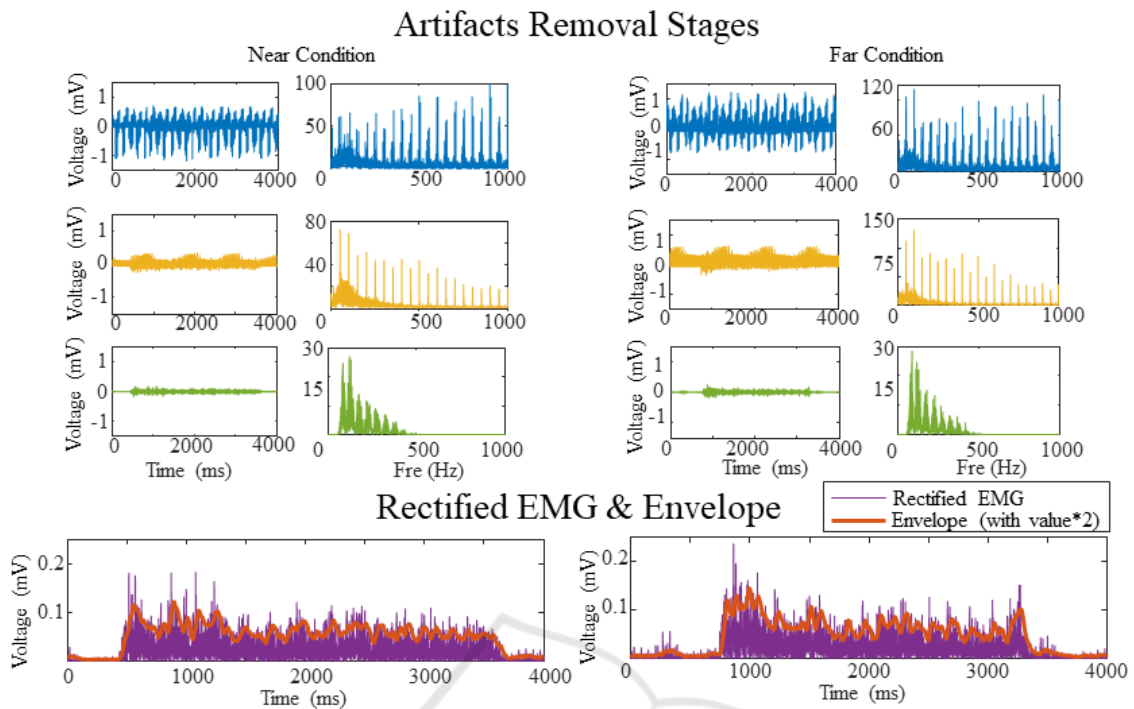


Figure 4: Extensor EMG signal and corresponding one-sided FFT spectrums at each processing stage. From top to bottom, the respective stages are raw EMG without blanking, EMG with hardware blanking, EMG with software filtering, and the final envelopes. The left and right columns are two cases where distance between stimulation and recording electrodes is near and far with each other, respectively.

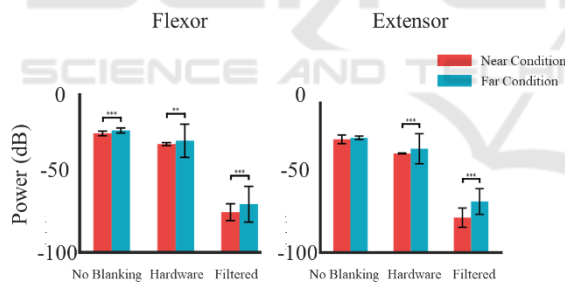


Figure 5: Bar plot of the harmonic power  $P_{stim}$  (mean  $\pm$  standard deviation) shows the average results of 3 able-bodied subjects across conditions. (Asterisks represent the statistically significant difference between the near and far intra-class conditions. \*\*,  $p < 0.01$ ; \*\*\*,  $p < 0.001$ ). Besides, all subjects show significant differences between different stages and different electrode placement conditions, which is not shown in the figure.

### 4.3 System Operation Validation Results

Figure 6 shows signals from both feedforward control and sensory feedback of the closed-loop prosthetic system.

It is shown that the difference between EMG envelopes of the flexor and the extensor increases

initially from zero to a positive value for hand closing, then jitters around dead zone, later decreases to a negative value for hand opening, and finally returns to zero at resting hand posture. This implies that control signals sent to the prosthetic hand first close the hand for grasping the object and then opens to release the object. This can also be seen from the plots of hand apertures at the bottom of Figure 6. It can be marked by several phases/timings ( $t_0$ ~ $t_5$ ). The  $t_0$  is the beginning of trial (waiting state). The  $t_1$  stands for the start of flexor recruitment by amputee for prosthesis operation. The EMG envelope difference rapidly increases as the prosthesis begins to close. The  $t_2$  stands for the timing that prosthetic fingers contact with the block, at which the prosthetic hand stops at the closing position, and the pressure starts to rise. The red arrow indicates the size identify response from the subject through ETS, and the period between  $t_3$  and  $t_1$  represents identification time. At the  $t_4$ , extensor contraction starts. However, the amplitude of EMG envelope difference between  $t_4$  and  $t_5$  fails to reach the level to drive the prosthesis, thus forming a dead zone. Then at hand opening stage  $t_5$ , the difference reverses to a sufficient value below 0. Finally, when the hand is fully open at  $t_6$ , contact pressure also drops along with the process.

During the hand closing phase, in the feedforward pathway the envelope difference is positive, corresponding to the subsequent rising in contact pressure and sensory feedback and vice versa. The correlations among these signals illustrate that the closed-loop system is functioning as expected in real-time in the grasping task.

Figure 7 shows the confusion matrix of size identification by the amputee subject. The accuracy of identification for VS, S, M, and L sizes are 100%, 90%, 80%, 90% respectively. It can be seen that in general the rate of misjudgement increased with the number of contacting digits. However, M size is the most likely one to be misjudged. This result confirms that grasping and perception can be performed ipsilaterally and simultaneously with the closed-loop control system.

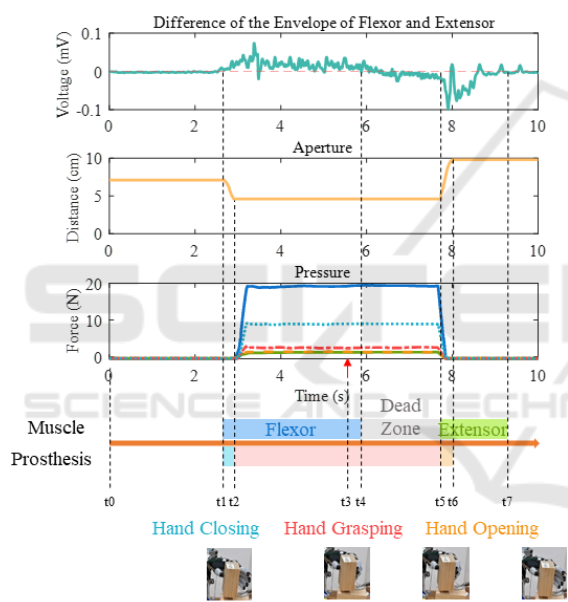


Figure 6: The illustration of the output signals by amputee and prosthesis phases during operation of the closed-loop control system. The bottom illustrates the change in prosthesis operation (hand apertures).

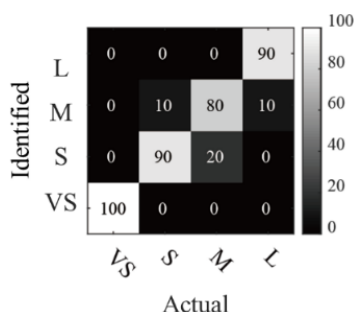


Figure 7: Confusion matrix presents the accuracy of size identification.

## 5 DISCUSSION AND CONCLUSION

This study applied a combination of hardware and software processing for artifact removal from TENS. The myoelectrical prosthetic hand can be integrated with the ETS-based sensory feedback in real-time for closed-loop control on ipsilateral side for amputees without data segment or artifact template database establishment. This enabled the user to operate the prosthetic hand to grasp objects and obtain sensory perception from specific fingers.

In order to remove stimulus artifacts caused by TENS with a relatively large amplitude of stimulation current, hardware circuitry of the EMG acquisition was modified to blank the output of EMG differential amplifiers in real-time triggered by stimulation pulses at each pulse delivery. Test indicated that this method eliminated part of stimulus artifacts, but allowed for maximum retention of EMG signals. In addition, digital filtering algorithms were adopted to remove remaining artifacts using a DSP. The difference of the envelopes of processed EMG signals was shown to be adequate as instructions to control the commercial prosthetic hand (Figure 6).

Results in Figure 5 indicate that stimulation electrodes placed farther away from the recording electrodes generated larger artifacts in the experiment of this study. This may be due to the fact that stimulus current trans-passed the recording electrodes. Thus, the longer the distance between stimulation and recording electrodes, the larger the volume resistance between them, yielding a larger stimulus artifact. In future applications, the reference electrodes for stimulation may be relocated to other places to further reduce the effect of stimulus artifacts.

Our study mainly shows that the receiving of sensory feedback and the control of prostheses can be integrated on ipsilateral side for amputees during TENS pulses delivering. The technique can be adequate to allow integrating myoelectric control of a commercial prosthetic hand with ETS-based sensory feedback, and can be further applied to other closed-loop systems with interference between pathways.

There is still room to improve signal processing methods. Other types of digital filters, such as Bayesian filters, could be employed for artifacts generated by higher stimulation frequencies. In addition, the amplitude of EMG envelopes varies with subjects and placement of EMG electrodes. Thus, in future applications, parameters of envelope gain should be adjustable according to each user for optimal closed-loop operation of control and sensory perception.

## ACKNOWLEDGEMENTS

This research was supported in part by a grant from Key-Area Research and Development Program of Guangdong Province (2020B0909020004), the National Key R&D Program of China (No. 2017YFA0701104, No. 2020YFC2007903), a grant from the National Natural Science Foundation of China (No. 81630050), and a grant from Science and Technology Commission of Shanghai Municipality (No. 20DZ2220400).

## REFERENCES

- Babb, T. L., Mariani, E., Strain, G. M., Lieb, J. P., Soper, H. V., & Crandall, P. H. (1978). A sample and hold amplifier system for stimulus artifact suppression. *Electroencephalography and Clinical Neurophysiology*, 44(4), 528–531.
- Bensmaia, S. J., Tyler, D. J., & Micera, S. (2020). Restoration of sensory information via bionic hands. *Nature Biomedical Engineering*, 1–13.
- Bi, Z.-Y., Zhou, Y.-X., Xie, C.-X., Wang, H.-P., Wang, H.-X., Wang, B.-L., Huang, J., Lü, X.-Y., & Wang, Z.-G. (2021). A hybrid method for real-time stimulation artefact removal during functional electrical stimulation with time-variant parameters. *Journal of Neural Engineering*, 18(4), 046028.
- Chai, G., Sui, X., Li, S., He, L., & Lan, N. (2015). Characterization of evoked tactile sensation in forearm amputees with transcutaneous electrical nerve stimulation. *Journal of Neural Engineering*, 12(6), 066002.
- Dosen, S., Schaeffer, M.-C., & Farina, D. (2014). Time-division multiplexing for myoelectric closed-loop control using electrotactile feedback. *Journal of NeuroEngineering and Rehabilitation*, 11.
- Frigo, C., Ferrarin, M., Frasson, W., Pavan, E., & Thorsen, R. (2000). EMG signals detection and processing for on-line control of functional electrical stimulation. *Journal of Electromyography and Kinesiology*, 10(5), 351–360.
- Hao, M., Chou, C.-H., Zhang, J., Yang, F., Cao, C., Yin, P., Liang, W., Niu, C. M., & Lan, N. (2020). Restoring Finger-Specific Sensory Feedback for Transradial Amputees via Non-Invasive Evoked Tactile Sensation. *IEEE Open Journal of Engineering in Medicine and Biology*, 1, 98–107.
- Johansson, R. S., & Flanagan, J. R. (2009). Coding and use of tactile signals from the fingertips in object manipulation tasks. *Nature Reviews Neuroscience*, 10(5), 345–359.
- Li, Y., Chen, J., & Yang, Y. (2019). A Method for Suppressing Electrical Stimulation Artifacts from Electromyography. *International Journal of Neural Systems*, 29(06), 1850054.
- Li, Y., Chou, C.-H., Zhang, J., Zhang, Z., Hao, M., & Lan, N. (2021). A Pilot Study of Multi-Site Simultaneous Stimulation for Tactile and Opening Information Feedback in the Prosthetic Hand. *2021 10th International IEEE/EMBS Conference on Neural Engineering (NER)*, 187–190.
- Liu, X. X., Chai, G. H., Qu, H. E., & Lan, N. (2015). A sensory feedback system for prosthetic hand based on evoked tactile sensation. *2015 37th Annual International Conference of the IEEE Engineering in Medicine and Biology Society (EMBC)*, 2493–2496.
- Pilkar, R., Ramanujam, A., Garbarini, E., & Forrest, G. (2016). Validation of empirical mode decomposition combined with notch filtering to extract electrical stimulation artifact from surface electromyograms during functional electrical stimulation. *2016 38th Annual International Conference of the IEEE Engineering in Medicine and Biology Society (EMBC)*, 1733–1736.
- Qiu, S., Feng, J., Xu, R., Xu, J., Wang, K., He, F., Qi, H., Zhao, X., Zhou, P., Zhang, L., & Ming, D. (2015). A Stimulus Artifact Removal Technique for SEMG Signal Processing During Functional Electrical Stimulation. *IEEE Transactions on Biomedical Engineering*, 62(8), 1959–1968.
- Rolston, J. D., Gross, R. E., & Potter, S. M. (2009). A Low-Cost Multielectrode System for Data Acquisition Enabling Real-Time Closed-Loop Processing with Rapid Recovery from Stimulation Artifacts. *Frontiers in Neuroengineering*, 2.
- Schauer, T., Salbert, R. C., Negard, N.-O., & Raisch, J. (2004). *Detection and Filtering of EMG for Assessing Voluntary Muscle Activity during FES*. 185–187.
- Smail, L. C., Neal, C., Wilkins, C., & Packham, T. L. (2021). Comfort and function remain key factors in upper limb prosthetic abandonment: Findings of a scoping review. *Disability and Rehabilitation: Assistive Technology*, 16(8), 821–830.
- Widjaja, F., Shee, C. Y., Poignet, P., & Ang, W. T. (2009). FES artifact suppression for real-time tremor compensation. *2009 IEEE International Conference on Rehabilitation Robotics*, 53–58.
- Yang, F., Hao, M.-Z., Zhang, J., Chou, C.-H., & Lan, N. (2020). An Experimental Protocol for Evaluating Pulse Width Modulation Ranges of Evoked Tactile Sensory Feedback in Amputees\*. *2020 42nd Annual International Conference of the IEEE Engineering in Medicine Biology Society (EMBC)*, 3869–3872.
- Yi, X., Jia, J., Deng, S., Shen, S. G., Xie, Q., & Wang, G. (2013). A Blink Restoration System With Contralateral EMG Triggered Stimulation and Real-Time Artifact Blanking. *IEEE Transactions on Biomedical Circuits and Systems*, 7(2), 140–148.
- Yochum, M., Bakir, T., Binczak, S., & Lepers, R. (2014). EMG artifacts removal during electrical stimulation, a CWT based technique. *2014 IEEE Region 10 Symposium*, 137–140.